

MEASUREMENTS OF RELATIVE PERMEABILITIES FOR WATER AND STEAM

Maria Gudjonsdottir^{1,2*}, Jonas Eliasson², Halldor Palsson², Gudrun Saevarsdottir¹

¹School of Science and Engineering, Reykjavik University, Menntavegur 1, IS-101 Reykjavik, Iceland

² School of Engineering and Natural Sciences, University of Iceland, Saemundargata 2, IS-101 Reykjavik, Iceland
*e-mail: msg@ru.is

ABSTRACT

Relative permeabilities are important parameters when determining the characteristics of two phase flow of geothermal fluids through porous reservoirs. When modeling such flow, several choices for relative permeability curves are available and thus they must be chosen by the modeler. This choice is however not always straightforward and results may differ quite a lot based on the selected curves.

To shed light on the applicability of different relative permeability curves, a measurement device has been designed and constructed which operates on a two phase mixture of water and steam for a specific pressure range. It has been used for measuring the necessary flow parameters needed to determine the relative permeabilities for different pressures, different flow directions and can be operated with different types of filling materials with different intrinsic permeability. The relative permeabilities were calculated according to Darcy's law in both vertical and horizontal setups from the measurements of the total mass flow of the two phases and their pressure gradients. The results are presented as experimental values of relative permeabilities for water and steam for different alignments in gravitational field.

INTRODUCTION

Understanding two phase flow of water and steam in porous media is important when exploiting geothermal reservoirs. When the flow of the two phases can be described by Darcy's law the concept of relative permeability is introduced. The simplest case of the relative permeability functions is the X-curve where they are equivalent to area reduction factors only. By using those curves, all interaction between the two phases are neglected. Previous research in the field of two phase flow in porous media has shown that interaction between the two phases as well as with the surrounding porous matrix must exist and the X-curve is not always applicable (Eliasson et al., 1980) (Mahiya, 1999) (O'Connor and

Horne, 2002) (Piquemal, 1994) (Satik, 1998) (Verma, 1986). A number of relative permeability curves are available from literature and they can be used to determine the relative permeabilities for water and steam in reservoir simulations (Pruess et al., 1999). Not much information is available about the effect of flow direction in a gravitational field on the relative permeabilities. Eliasson et.al (1980) conducted measurements where a mixture of water and steam was injected into a vertically aligned cylinder. The results indicated that the dominant phase may assist the flow of the other phase thus increasing the relative permeability of the non-dominant phase. This fact is the motivation for the project described in this paper. The main goal of this research is to compare the flow of water and steam when flowing in different directions under the influence of gravity. A measurement device has been designed, constructed and installed and preliminary measurements of two phase flow of water and steam through the device have been conducted.

THEORETICAL BACKGROUND

The governing equations which can describe the two phase flow of water and steam in porous media are determined from the flow region to which the flow belongs. The Darcy's law is applicable for a laminar flow with low Reynolds numbers (Re). For higher Reynolds number the Darcy Forchheimer relations apply. A summary of these theoretical and empirical relations follows.

The Darcy's Law for Single Phase Flow

The Darcy's law describes the flow of a fluid through a porous media (Darcy, 1856). For the Darcy's law to apply, certain conditions have to be fulfilled, the flow has to be laminar and flow with low velocity. The Darcy's law is valid for a fluid flow if $Re < 1$, however it has been shown that this limit can be extended to $Re = 10$ (Todd and Mays, 2005). The Reynolds number for flow in porous media is defined as shown in Eq. (1) (Chilton and Colburn, 1931):

$$Re = \frac{ud}{v} \quad (1)$$

where u is the velocity of the fluid, in this case defined as the Darcy velocity or discharge per unit area (Todd and Mays, 2005), ν is the fluids kinematic viscosity and d is the representative grain size diameter defined as a certain passing sieve diameter. Different values for the passing sieve diameter to be used in Eq. (1) can be found in literature, normally ranging between 10-30%, meaning, that d is the sieve diameter when 10-30% of the grains have passed the sieve.

The Darcy's law for a single phase flow is shown in Eq. (2).

$$\bar{q} = -\frac{k}{\nu}(\nabla p - \rho \bar{g}) \quad (2)$$

where \bar{q} is the mass flux (mass flow per unit area) of the fluid, k is the intrinsic permeability of the porous matrix, ν is the kinematic viscosity of the fluid, ∇p is the pressure gradient the fluid experiences, ρ is the fluid density and \bar{g} is the gravitational acceleration.

When conducting experiments of flow in porous media it can be more convenient to use the mass flow definition from Eq. (3).

$$\bar{m} = -\frac{k}{\nu}A(\nabla p - \rho \bar{g}) \quad (3)$$

where A is the area of the porous flow channel. Eqs (2) and (3) apply for a single phase flow where there is only one phase flowing through the permeable matrix such as in groundwater applications.

The Darcy's Law for Two Phase Flow

Where there are two phases flowing through the porous matrix as can be the case in e.g. oil and gas reservoirs and geothermal reservoirs the Darcy's law from Eq. (3) is not sufficient to describe the flow. Thus, two equations are introduced with permeability reduction factors for each phase, called relative permeabilities. The Darcy's law for two phase flow is shown in Eqs (4) and (5) where the two phases used here are water (subscript w) and steam (subscript s).

$$\bar{m}_w = -\frac{kk_{rw}}{\nu_w}A(\nabla p - \rho_w \bar{g}) \quad (4)$$

$$\bar{m}_s = -\frac{kk_{rs}}{\nu_s}A(\nabla p - \rho_s \bar{g}) \quad (5)$$

Here, k_{rs} and k_{rw} are the relative permeabilities for steam and water respectively. For determining if two phase flow obeys the Darcy's law the corresponding Reynolds number from Eq. (1) has to be estimated. The mixture properties must also be determined, but there are different methods available to calculate the kinematic viscosity ν_t , of a two phase mixture. The kinematic viscosity is determined from:

$$\nu_t = \frac{\mu_t}{\rho_t} \quad (6)$$

where μ is the fluid dynamic viscosity and the subscript t indicates a mixture. The density of the mixture is determined from the mass balance of the two phases and is shown in Eq. (7).

$$\rho_t = \left(\frac{x}{\rho_s} + \frac{1-x}{\rho_w}\right)^{-1} \quad (7)$$

where x is the mass fraction of steam in the total flow (also called steam fraction) and is defined with Eq. (8).

$$x = \frac{\dot{m}_s}{\dot{m}_w + \dot{m}_s} \quad (8)$$

where \dot{m}_s and \dot{m}_w represent the steam and the water mass flows respectively. For determining the total viscosity of the two phase mixture, μ_t , various expressions are available from literature (Awad and Muzychka 2008), examples of that are shown in Eq. (9) (McAdams et al., 1942) and Eq. (10) (Cicchitti et al., 1960).

$$\mu_t = \left(\frac{x}{\mu_s} + \frac{1-x}{\mu_w}\right)^{-1} \quad (9)$$

$$\mu_t = x\mu_s + (1-x)\mu_w \quad (10)$$

If the relative permeabilities of the phases are known and the flow obeys the Darcy's law, the total kinematic viscosity of the mixture can be determined as shown in Eq. (11) and the total enthalpy, h_t , of the mixture as shown in Eq. (12).

$$\nu_t = \left(\frac{k_{rw}}{\nu_w} + \frac{k_{rs}}{\nu_s}\right)^{-1} \quad (11)$$

$$h_t = \nu_t \left(h_w \frac{k_{rw}}{\nu_w} + h_s \frac{k_{rs}}{\nu_s}\right) \quad (12)$$

where h_w and h_s are the saturation enthalpies for water and steam respectively. Here Eqs (13) and (14) were used to gain Eqs (11) and (12) for one dimensional horizontal flow.

$$\dot{m}_t = \dot{m}_w + \dot{m}_s = -\frac{k}{\nu_t}A \frac{dp}{dx} = -\frac{kk_{rw}}{\nu_w}A \frac{dp}{dx} - \frac{kk_{rs}}{\nu_s}A \frac{dp}{dx} \quad (13)$$

$$\dot{m}_t h_t = -\frac{k}{\nu_t}A \frac{dp}{dx} h_t = -\frac{kk_{rw}}{\nu_w}A \frac{dp}{dx} h_w - \frac{kk_{rs}}{\nu_s}A \frac{dp}{dx} h_s \quad (14)$$

These mixture properties are therefore highly depending on the relative permeabilities (Bodvarsson et al. 1980).

Non Darcy Flow

For flow with higher Reynolds numbers the Darcy's law is not sufficient alone and a correction factor has to be added to the equation and the flow in porous media is determined by the Forchheimer equation (Forchheimer, 1901) (Zeng and Grigg, 2006):

$$-\frac{dp}{dx} = \frac{\mu v}{k} + \beta \rho v^2 \quad (15)$$

Where dp/dx is the one dimensional pressure gradient and β is the inertial coefficient.

Energy Equations

When the pressure of a high enthalpy fluid is reduced below its saturation point flashing will occur. In the case of water, the amount of steam (steam fraction) resulting from the flashing process can be determined with Eq. (16).

$$x = \frac{h_t - h_w}{h_s - h_w} \quad (16)$$

For flow where heat losses, \dot{q} , occur, the energy balance between two points 1 and 2 in the flashing process can be expressed as:

$$h_1 + \frac{v_1^2}{2} + gz_1 = h_2 + \frac{v_2^2}{2} + gz_2 + \dot{q} \quad (17)$$

where h is the fluid enthalpy, $\frac{v^2}{2}$ the fluid kinetic energy and gz the potential energy.

Definition of Water Saturation

The relative permeabilities for water and steam are normally presented as two different functions of the local (in-place) water saturation as demonstrated in Eqs (18) and (19).

$$k_{rw} = f(S_w) \quad (18)$$

$$k_{rs} = g(S_w) \quad (19)$$

The functions f and g can be found by experiments. The local water saturation of a steady state flow is defined from the volume fraction of the water phase as seen in Eq. (20) and for one dimensional flow as in Eq. (21).

$$S_w = \frac{V_w}{V_w + V_s} \quad (20)$$

$$S_w = \frac{A_w}{A_w + A_s} \quad (21)$$

Where V_w and V_s are the water and steam volumes and A_w and A_s the areas of the flow channel occupied by the water and the steam phase respectively. When determining the relative permeabilities for geothermal reservoirs it can be difficult to measure the local water saturation. The flowing saturation however, $S_{w,f}$ can be used.

$$S_{w,f} = \frac{(1-x)v_w}{(1-x)v_w + xv_s} \quad (22)$$

Where v_w and v_s are the specific volumes of water and steam respectively. These two saturations (local and flowing) can be different for the same flow case (Reyes et al. 2004), (Shinohara 1978).

Relative Permeability curves

Several relations for the relative permeabilities as functions of the local steam saturation are available in the literature and presented as functions, see Eqs. (18) and (19). They have been gained from previous experiments and some of them which can be selected in the TOUGH2 reservoir simulator (Pruess et al. 1999) are listed in Table 1. In Table 1 the relative permeabilities are presented as functions of the normalized saturation, S_{wn} , which is defined as the saturation for the mobile region of the two phases. The normalized saturation can be related to the local saturation as shown in Eq. (23), accompanied by the residual saturations S_{wr} and S_{sr} for water and steam respectively. The residual saturation is the minimal saturation value the phase has to reach to become mobile.

$$S_{wn} = \frac{S_w - S_{wr}}{1 - S_{wr} - S_{sr}} \quad (23)$$

Table 1: A number of relative permeability curves used in the TOUGH2 reservoir simulator (Pruess et al. 1999)

Name	$k_{rw} = f(S_{wn})$	$k_{rs} = g(S_{wn})$
X-Curves	$k_{rw} = S_{wn}$	$k_{rs} = 1 - S_{wn}$
Corey curves (Corey, 1954)	$k_{rw} = S_{wn}^4$	$k_{rs} = (1 - S_{wn})^2(1 - S_{wn}^2)$
Grant's curves (1977)	$k_{rw} = S_{wn}^4$	$k_{rs} = 1 - k_{rw}$
Functions of Fatt and Klikoff (1959)	$k_{rw} = S_{wn}^3$	$k_{rs} = (1 - S_{wn})^3$
Functions of Verma et al. (1985)	$k_{rw} = S_{wn}^3$	$k_{rs} = 1.259 - 1.7615S_{wn} + 0.5089S_{wn}^2$

METHOD

In this research the relative permeabilities are determined for different flow conditions and different flow directions. It was decided to build a relatively large flow channel to minimize end effects at wall and ends and to design the equipment so that it could withstand high pressure and temperature (up to 20 bar_g with a corresponding saturation temperature of 215°C).

Measurement Device

A 10" diameter and 4 m long seamless steel pipe was selected for this purpose and installed inside the separator station at Reykjanes geothermal power plant. The main design parameters of the pipe are listed in Table 2 and a simplified schematic representation of the pipe shown in Fig. 1. Also shown are the positions of pressure sensors located on the pipe. The pressure measurements are used to estimate pressure gradients needed for the relative permeability calculations.

Table 2: Main technical specifications of the material used in the measurement device

Pipe material	P235GH	
Pipe outer diameter	273	mm
Pipe thickness	5	mm
Pipe length	4	m
Flanges	10" Class 600	
Filling	Crushed basalt	0-2mm

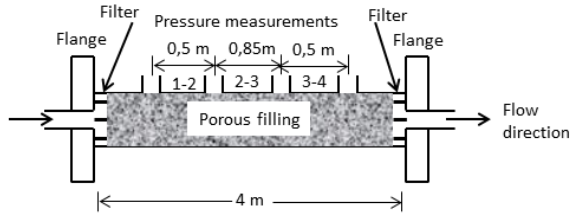


Figure 1: Placement of pressure sensors on the measurement device (pipe)

Saturated water from steam separators in the power plant was available at 18.6 bar_g and used to produce a two phase mixture by flashing the water through a throttle valve. By reducing the opening of the valve, the pressure decreases and the steam quality increases. Thereby, a range of inlet pressure into the device could be used in the experiments.

A simplified process diagram for the device is shown in the left hand side of Fig. 2 and a photo showing the experimental setup is shown on the right hand side in Fig.2.

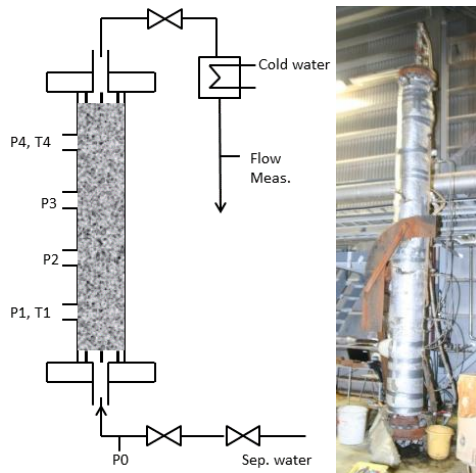


Figure 2: Left: Process diagram of the measurement device. Right: Photo showing the experimental setup

The pressure was measured at 5 different locations on the device as indicated in Fig. 2. One pressure indicator was located at the inlet (P0 in Fig. 2) and one pressure indicator and one pressure sensor at every location, denoted as P1-P4 in Fig. 2. Additionally, two temperature sensors were located on the device, one at same place as P1 and the other at the same place as P4. The pressure sensors were connected to a power supply and they produced 4-20 mA signals for the range of 0-25 bar_g. in a circuit. An electrical resistance was connected into the circuit and the voltage difference over the resistance was read with an AD converter and logged with the LabVIEW Signal Express® software. The pressure

indicators were used for redundancy of the pressure sensors. The temperature sensors were thermocouples K-type. The filling material inside the pipe was sand, mainly crushed basalt with grain size 0-2 mm and a 30% passing sieve diameter of 0.25 mm.

Measurements

Intrinsic Permeability

After the steel pipe was filled with the sand it was sealed and the intrinsic permeability could be calculated from measurements using water flowing through the porous filling. The pressure drop along the pipe as well as the mass flow was measured and the intrinsic permeability calculated according to Eq. (2). Condensed water from the Reykjanes power plant was available with up to 20 bar_g pressure and used for measuring the intrinsic permeability for a range of inlet pressures. The condensed water has a temperature of 40°C and flows from the turbine and the condenser exits from the power plant. The water was injected at a given flow rate into the pipe and pressure of the fluid was measured at four different locations on the pipe as seen in Figs 1 and 2. The intrinsic permeability could therefore be measured for different intervals of the flow path. Six different intervals could be defined for the pressure gradient calculations as listed in Table 3.

Table 3: Definition of intervals used for the calculation of pressure gradient

Interval	Pressure measurements	Interval length
1 – 2	P1-P2	0.5 m
2 – 3	P2-P3	0.85 m
3 – 4	P3-P4	0.5 m
1 – 3	P1-P3	1.35 m
1 – 4	P1-P4	1.85 m
2 – 4	P2-P4	1.35 m

Relative Permeabilities

To conduct measurements for the calculation of the relative permeabilities the device needed to be heated up gradually to reach steady conditions for a given inlet pressure. When steady state conditions (pressure, flow and temperature) were met, the pressure gradient was measured as well as the total flow. The steam fraction at each pressure port was calculated with Eq. (16) and the mass flow of each phase calculated from the steam fraction x and the total mass flow \dot{m}_t according to following Eqs (24) and (25).

$$\dot{m}_w = (1 - x)\dot{m}_t \quad (24)$$

$$\dot{m}_s = x\dot{m}_t \quad (25)$$

Eqs. (4) and (5) were then used to determine the relative permeabilities k_{rw} and k_{rs} . The heat losses were estimated from convection heat transfer and accounted for in Eq. (17). The Reynolds number from Eq. (1) was calculated and did not exceed the upper limit ($Re=10$) and therefore the flow was considered to be in the laminar regime.

RESULTS

Intrinsic Permeability

Table 4 shows the results of the measurements of intrinsic permeability when the condensed water was flowing through the porous filling inside the pipe. The intrinsic permeability could be measured for each interval between every two pressure ports, thus resulting in six different values for each flow case as defined in Table 3. The intrinsic permeability was measured at different times during the experiments, which are here presented as case A, B and C as follows:

Case A: Initial run after filling, vertical alignment

Case B: After approximately 20 hours of running two phase mixture through the device, vertical alignment

Case C: Horizontal alignment after changing from vertical alignment

It is clear from those results shown in Table 4 that the intrinsic permeability is not constant for all the intervals. This variation in the values may be the result of shifting in the packing of the sand particles which were used as the filling material. The fluid used for the two phase measurements is separated water from the power plant in Reykjanes power plant. That fluid is high in silica content and the silica may precipitate on the sand particles as its pressure reduces and therefore reduce the permeability gradually.

The intrinsic permeability between pressure ports 1 and 4 is nevertheless similar for all the three flow cases and that interval is therefore a good candidate for comparison between the horizontal and the vertical alignment.

Table 4: Measured intrinsic permeability values for different intervals on the device

Interv.	Case	k [D]	Interv.	Case	k [D]
1 - 2	A	5.0	2 - 3	A	4.2
1 - 2	B	5.5	2 - 3	B	2.8
1 - 2	C	7.3	2 - 3	C	2.7
3 - 4	A	4.8	1 - 3	A	4.4
3 - 4	B	17.2	1 - 3	B	3.5
3 - 4	C	15.4	1 - 3	C	3.5
2 - 4	A	4.4	1 - 4	A	4.5
2 - 4	B	4.0	1 - 4	B	4.3
2 - 4	C	4.0	1 - 4	C	4.5

Relative Permeabilities

Normally the calculated relative permeabilities from measurements are presented as functions of the measured local saturation as shown in Eqs (18) and (19). In the experiments described here, the local saturation was not measured but in order to compare the results of the relative permeabilities with values from previous research, they are plotted on the same graph with the water relative permeability on the x-axis and the steam relative permeability on the y-axis. Figs 3 and 6 show the resulting relative permeabilities together with selected curves from Table 1 for comparison. This was done for both the vertical and horizontal flow alignments and can be seen in Figs 3 and 6. Also the flowing saturation $S_{w,f}$ from Eq. (22) was calculated and the relative permeabilities plotted as functions of $S_{w,f}$. Those graphs are shown in Figs 4 and 5 for vertical flow direction and in Figs 7 and 8 for horizontal flow direction.

Vertical Flow Direction

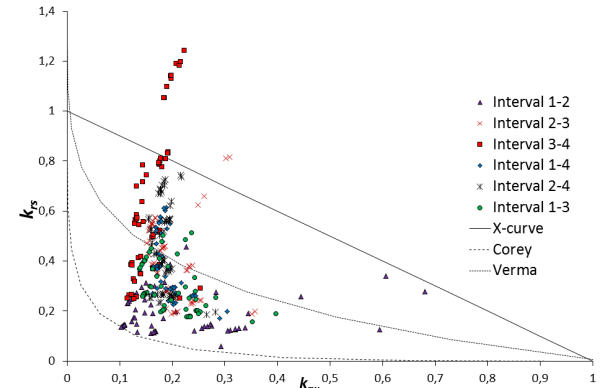


Figure 3: The relative permeabilities plotted on the same graph for vertical flow alignment

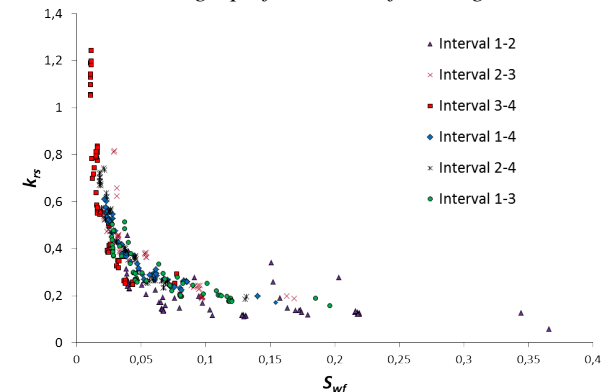


Figure 4: The relative permeabilities for steam vs. the flowing saturation for vertical flow direction

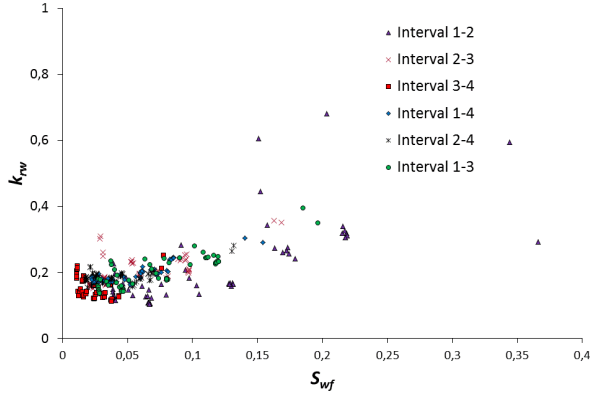


Figure 5: The relative permeabilities for water vs. the flowing saturation for vertical flow direction

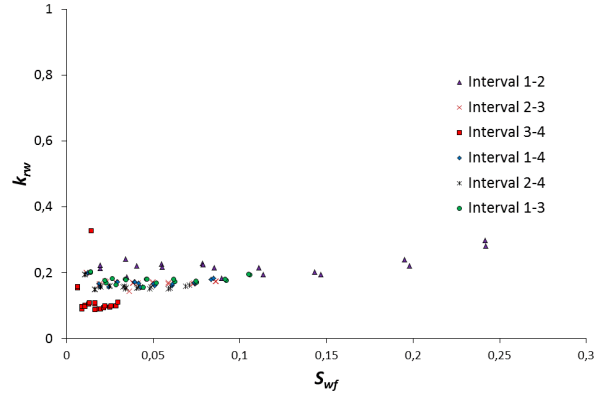


Figure 8: The relative permeabilities for water vs. the flowing saturation for horizontal flow direction

Horizontal Flow Direction

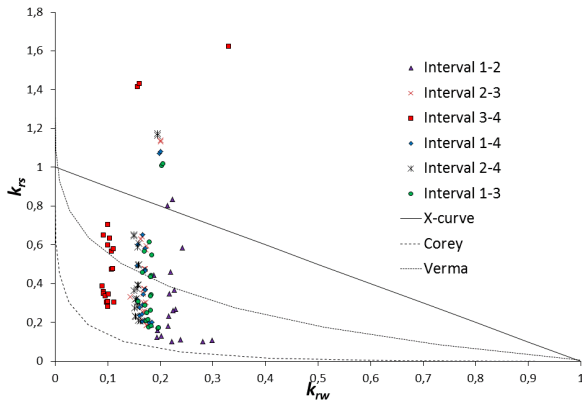


Figure 6: The relative permeabilities plotted on the same graph for horizontal flow direction

Comparison of Flow Directions

In Figs 9, 10 and 11 the results are compared for the horizontal and the vertical flow alignment for the interval 1-4 shown in Fig. 1.

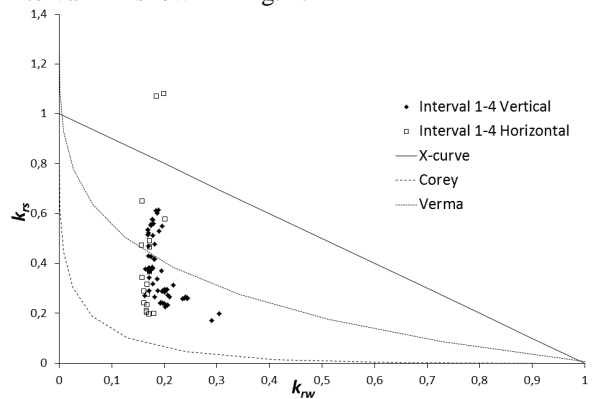


Figure 9: The relative permeabilities plotted on the same graph for the same interval in vertical and horizontal flow direction

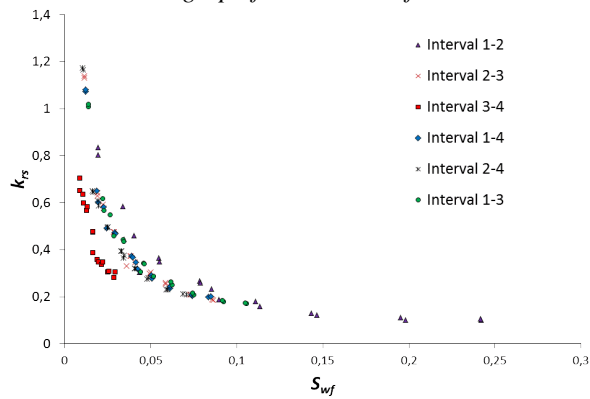


Figure 7: The relative permeabilities for steam vs. the flowing saturation for horizontal flow direction

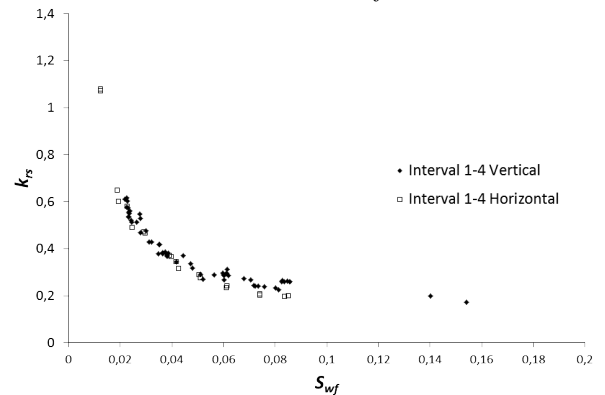


Figure 10: The relative permeabilities for steam vs. the flowing saturation for vertical and horizontal flow alignment for the interval 1-4

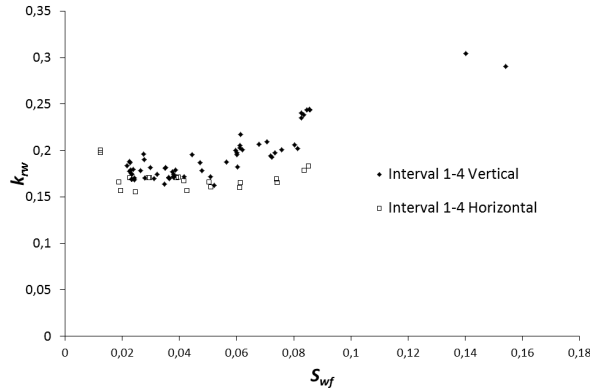


Figure 11: The relative permeabilities for water vs. the flowing saturation for vertical and horizontal flow alignment for the interval 1-4

DISCUSSION

Since the intrinsic permeability did not appear to remain constant for all the intervals it is questionable if all the intervals in the pipe are comparable as seen in Figs 3 and 6. However, by looking at interval 1-4 in Fig. 9 it appears that for the vertical alignment the relative permeabilities show a curvilinear pattern for higher water content but as the steam content increases the measured points deviate from that curve. For horizontal alignment the measured points do not follow that pattern and the relative permeability for water seems to be constant for a broad range of steam relative permeabilities. These values have only be measured for a narrow range of flowing saturation $S_{w,f}$. Further experiments are needed to investigate this and changes may have to be made on the experimental device. It might be the case that the water is collected at the bottom of the pipe in the horizontal alignment since the inlet and the exit are located at the center axis of the pipe. When looking at Fig. 4 the steam relative permeability for the vertical flow direction follows a pattern for all the data points whereas for the horizontal case two different patterns may be observed on Fig. 7. For the water relative permeability in Fig. 5 (vertical flow direction) a pattern can be observed and the water relative permeability seems to increase for low water content, indicating that the steam is enhancing the water flow and thereby indicating that the water is pushed upwards by the steam. This however is not as clear for the horizontal flow case, as seen in Fig. 8, but when looking at one interval in Fig. 11 this interaction can be observed as the water permeabilities increase for smaller flowing saturations $S_{w,f}$.

CONCLUSION

The results shown in this paper are the first results from the measurements made using the device described in the paper. They indicate that the relative permeabilities for the horizontal and vertical flow directions can be different. It is clear though that further research is needed to verify this result.

ACKNOWLEDGEMENTS

This research has received financial support from Energy Research Fund of Landsvirkjun, the Geothermal Research Group (GEORG) in Iceland and University of Iceland Equipment Fund. Their contribution is highly appreciated.

REFERENCES

- Awad, M.M., Muzychka, Y.S. (2008), "Effective Property Models for Homogeneous Two-Phase Flows," *Experimental Thermal and Fluid Science*, 33, 106-113.
- Bodvarsson, G.S., O'Sullivan, M.J. and Tsang, C.F. (1980) "The Sensitivity of Geothermal Reservoir Behavior to Relative Permeability Parameters," *Proc., 6th Workshop on Geothermal Reservoir Engineering, Stanford*.
- Chilton, T.H. and Colburn, A.P. (1931), "Pressure Drop in Packed Tubes," *Industrial and Engineering Chemistry*, 23, 913-919.
- Cicchitti, A., Lombaradi, C., Silversti, M., Soldaini, G., Zavattarlli, R. (1960), "Two-Phase Cooling Experiments – Pressure Drop Heat Transfer Burnout Measurements," *Energia Nucleare*, 7, 407-425.
- Corey, A.T. (1954), "The Interrelation Between Gas and Oil Relative Permeabilities". *Producers Monthly*, 38-41.
- Darcy, H. (1856), "Les fontaines publiques de la ville de Dijon", Dalmont, Paris.
- Eliasson, J., Kjaran S.P., Gunnarsson G. (1980), "Two phase flow in porous media and the concept of relative permeabilities". *Proc., 6th Workshop on Geothermal Reservoir Engineering, Stanford*.
- Fatt, I. and Klikoff W.A. (1959), "Effect of Fractional Wettability on Multiphase Flow Through Porous Media," *AIME Transactions*, 216-246.
- Forchheimer, P. (1901) "Wasserbewegung Durch Boden", *Verein Deutscher Ingenieure*, 45, 1781-1788.

- Grant, M.A. (1977), "Permeability Reduction Factors at Wairakei," *Paper 77-HT-52, presented at AICHE-ASME, Heat Transfer Conference, Salt Lake City, Utah.*
- Mahiya, G. (1999), "Experimental Measurement of Steam-Water Relative Permeability," *M.Sc. Thesis, Stanford University, California.*
- McAdams, W.H., Woods, W.K., Heroman, I.C. (1942), "Vaporization Inside Horizontal Tubes II-Benzene-Oil Mixtures," *Trans. ASME*, 64 (3), 193-200.
- O'Connor, P.A., Horne R. (2002), "Constant-Pressure Measurement of Steam-Water Relative Permeability," *Proc., 27th Workshop on Geothermal Reservoir Engineering, Stanford.*
- Piquemal, J. (1994), "Saturated Steam Relative Permeabilities of Unconsolidated Porous Media," *Transport in Porous Media* 17:105-120.
- Pruess, Karsten, Oldenburg C., Moridis G. (1999), "TOUGH2 User's Guide, Version 2.0," *Earth Sciences Division, Lawrence Berkeley National Laboratory, University of California, Berkeley.*
- Reyes, J.L.P., Chen, C—Y., Li, K. and Horne, R.N. (2004) "Calculation of Steam and Water Relative Permeabilities Using Field Production Data, With Laboratory Verification," *Geothermal Resources Council Transactions*, 28, 609-615.
- Satik, C. (1998), "A Measurement of Steam-Water Relative Permeability," *Proc., 23rd Workshop on Geothermal Reservoir Engineering, Stanford.*
- Shinohara, K. (1978), "Calculation and Use of Steam/Water Relative Permeabilities in Geothermal Reservoirs," *MS report, Stanford University, Stanford, California.*
- Todd, D. K. and Mays, L.W. (2005), "Groundwater Hydrology," *Third Edition. John Wiley and Sons, Inc.*
- Verma, A.K. (1986), "Effects of Phase Transformation of Steam-Water Relative Permeabilities," *Ph.D. Thesis. University of California, Berkeley.*
- Zeng, Z., Grigg, R. (2006), "A Criterion for non-Darcy Flow in Porous Media," *Transport in Porous Media*, 63, 57-69.